Electrical waves in a one-dimensional model of cardiac tissue

Margaret Beck*, Christopher K. R. T. Jones†, David Schaeffer‡, and Martin Wechselberger§

July 7, 2008

Abstract

The electrical dynamics in the heart is modeled by a two-component PDE. Using geometric singular perturbation theory, it is shown that a traveling pulse solution, which corresponds to a single heartbeat, exists. One key aspect of the proof involves tracking the solution near a point on the slow manifold that is not normally hyperbolic. This is achieved by desingularizing the vector field using a blow-up technique. This feature is relevant because it distinguishes cardiac impulses from, for example, nerve impulses. Stability of the pulse is also shown, by computing the zeros of the Evans function. Although the spectrum of one of the fast components is only marginally stable, due to essential spectrum that accumulates at the origin, it is shown that the spectrum of the full pulse consists of an isolated eigenvalue at zero and essential spectrum that is bounded away from the imaginary axis. Thus, this model provides an example in a biological application reminiscent of a previously observed mathematical phenomenon: that connecting an unstable – in this case marginally stable – front and back can produce a stable pulse. Finally, remarks are made regarding the existence and stability of spatially periodic pulses, corresponding to successive heartbeats, and their relationship with alternans, irregular action potentials that have been linked with arrhythmia.

1 Introduction

The first model of electrical activity in the cardiac membrane, an adaptation of the classic Hodgkin-Huxley model of neural dynamics, was introduced by Noble [HN60, Nob62] for the Purkinje fiber. Beeler and Reuter [BR77] introduced the first model for the dynamics of a ventricular myocyte, and more complicated models including additional and new experimental data (see, for example, Luo and Rudy [LR91, LR94]) followed. The main aim of all these models was to describe generic restitution properties of cardiac tissue, as well as to support spiral waves that break up spontaneously. Restitution refers to the relation between the diastolic interval, the interval between the end of an action potential and the beginning of the next action potential, and the duration of the next action potential pulse. The length and shape of action potentials in myocardial cells are distinct from those of the Hodgkin-Huxley model. In particular, myocardial cells have substantially prolonged action potentials, compared to neural action potentials, which facilitates muscular contraction. See figure 1a.

*University of Surrey, Guildford GU2 7XH, UK, M.Beck@surrey.ac.uk

†University of North Carolina, Chapel Hill, NC 27599, USA, ckrtj@email.unc.edu, and University of Warwick, Coventry CV4 7AL, UK, C.K.R.T.Jones@warwick.ac.uk

‡Duke University, Durham, NC 27708, USA, dgs@math.duke.edu

§University of Sydney, NSW, 2006, Australia, wm@maths.usyd.edu.au

In order to focus on the qualitative aspects of the Hodgkin-Huxley model of membrane activity in the giant squid axon, a simplified version, known as the FitzHugh-Nagumo model, was developed. In the same spirit, Karma [Kar93, Kar94] extracted a model of minimal complexity that reproduces restitution properties of the above mentioned cardiac cell models. Because these properties are absent in the standard FitzHugh-Nagumo model, it was necessary to introduce a different minimal model.

In this paper, we study a variant of Karma's model that was introduced by Mitchell and Schaeffer [MS03]. In addition, we allow for spatial variation and replace the step functions that appear in their model by smooth functions. The result is

$$\begin{aligned} v_t &= \kappa v_{xx} + I_{in}(v,h) + I_{out}(v) + I_{stim}(t)\,, \\ h_t &= \frac{h_\infty(v) - h}{\tau_h(v)}, \end{aligned} \tag{1.1}$$

where

$$I_{in}(v,h) = \frac{1}{\tau_{in}} h v^2 (1-v), \quad I_{out}(v) = -\frac{1}{\tau_{out}} v,$$

$$h_\infty(v) = \begin{cases} 1 & \text{if } v < v_{crit} - \delta_v \\ f^h(v) & \text{if } v_{crit} - \delta_v < v < v_{crit} + \delta_v \\ 0 & \text{if } v_{crit} + \delta_v < v \end{cases},$$

and

$$\tau_h(v) = \begin{cases} \tau_{open} & \text{if } v < v_{crit} - \delta_v \\ f^\tau(v) & \text{if } v_{crit} - \delta_v < v < v_{crit} + \delta_v \\ \tau_{close} & \text{if } v_{crit} + \delta_v < v \end{cases}.$$

where δ_v is sufficiently small, f^h and f^τ are smooth, monotonic functions that give continuity of the functions h_∞ and τ_h, and $I_{stim}(t)$ is an external stimulus. In the above equations, $x \in \mathbb{R}$, $t > 0$, $v = v(x,t) \in \mathbb{R}$ corresponds to the membrane potential of myocardial tissue and $h = h(x,t) \in \mathbb{R}$ is a gating variable. Both are dimensionless quantities that can range between zero and one.

The change of membrane potential v is governed by diffusion, through the diffusion coefficient κ, and the ionic currents. The current $I_{in}(v,h)$ denotes a bulk inward current, a combination of all currents that raise the voltage accross the membrane – primarly sodium and calcium current. This current is voltage dependent and includes the gating variable h – open when $h = 1$, closed when $h = 0$ – that governs the inactivation of the bulk inward current. The current $I_{out}(v)$ denotes a bulk outward current, a combination of all currents that decreases the voltage across the membrane – primarly potassium current. This current is voltage dependent but ungated. The stimulus current I_{stim} is an external current usually applied in brief pulses, either by a pacemaker cell or an experimenter.

The parameters τ_{in} and τ_{out} govern the flow of ions into and out of the cell, respectively, and the parameters τ_{open} and τ_{close} govern the opening and closing rates of the gate h. Based upon physiological information, it is reasonable to assume that

$$\tau_{in},\ \tau_{out} \ll \tau_{open},\ \tau_{close}. \tag{1.2}$$

Therefore, changes in the voltage v occur much faster than changes in the gating variable h, the inactivation of the bulk inward current. We exclude the case where the speed τ_{out} of the bulk outward current is comparable to the speeds of the gating variable h. For a myiocardial cell to be able to produce an action potential, it is a necessary to have $\tau_{out}/\tau_{in} := R$ sufficiently large, i.e. activation must occur before

deactivation - the inward current has to be sufficiently faster than the outward current. The exact minimal size for R is dependent on the specific model, and we will see below that for the model we investigate it is $R > 4$. Similar conditions on the gating speeds are not necessary for the existence of action potentials. We remark that, although R is large, it is not asymptotically large with respect to $1/\epsilon$, where ϵ is a small parameter that we define below.

Under these assumptions we will rescale space and time so that

$$\kappa = 1, \quad \tau_{out} = 1, \quad 1/\tau_{in} = R. \tag{1.3}$$

We remark that it is not necessary that $\tau_{open} = \tau_{close}$, but we assume this for convenience. Allowing them to differ, but remain of the same order, would only change the decay/growth rates on the slow manifold and would not qualitatively affect our results. Therefore, we define ϵ via

$$1/\tau_{open} = 1/\tau_{close} = \epsilon. \tag{1.4}$$

We note that similar scalings were used in [MS03]. For typical values of these parameters, see [CS06]. The relevance of different choices of R will be discussed further, below. The voltage threshold v_{crit} determines when the gate switches from an opening to a closing state or vice versa, and it is reasonable to assume that $0 < v_{crit} < 1/2$ [MS03, CS06].

In this paper, we will be primarily interested in traveling pulse solutions, corresponding to a single heartbeat, stimulated in the distant past at $x = -\infty$. The reason for this is the following. One particularly interesting biological behavior, found in the ODE version of the model, is a bifurcation in the response to periodic external stimulation as the frequency is increased. For smaller frequencies, the model produces action potentials with constant maximum value in one-to-one correspondence with the stimulus. As the frequency increases, this behavior can destabilize and alternans, action potentials with beat to beat variation in their restitution, can appear. This phenomenon has been linked with ventricular fibrillation and sudden cardiac death [CS06]. In order to eventually understand this phenomenon in spatially dependent models, we first seek to understand the dynamics of a single heartbeat, which is described by a traveling pulse solution to the above model without external stimulus. Therefore, in this paper we will set $I_{stim}(t) \equiv 0$.

Thus, the model we will study throughout is

$$\begin{aligned} v_t &= v_{xx} + Rhv^2(1-v) - v \\ h_t &= \epsilon g(v,h), \end{aligned} \tag{1.5}$$

where

$$g(v,h) = \begin{cases} 1-h & \text{if } v < v_{crit} - \delta_v \\ f^h(v) - h & \text{if } v_{crit} - \delta_v < v < v_{crit} + \delta_v \\ -h & \text{if } v_{crit} + \delta_v < v, \end{cases} \tag{1.6}$$

and we have chosen $f^\tau(v) = 1/\epsilon = \tau_{open} = \tau_{close}$. Notice that $(v,h) \equiv (0,1)$ is a stationary solution of equation (1.5). We are interested in traveling pulses that are biasymptotic to this stationary solution. In order to study such solutions, we define the moving coordinate $\xi = x + ct$ and analyze the model in the (ξ, t) coordinates:

$$\begin{aligned} v_t &= v_{\xi\xi} - cv_\xi + Rhv^2(1-v) - v \\ h_t &= -ch_\xi + \epsilon g(v,h). \end{aligned} \tag{1.7}$$

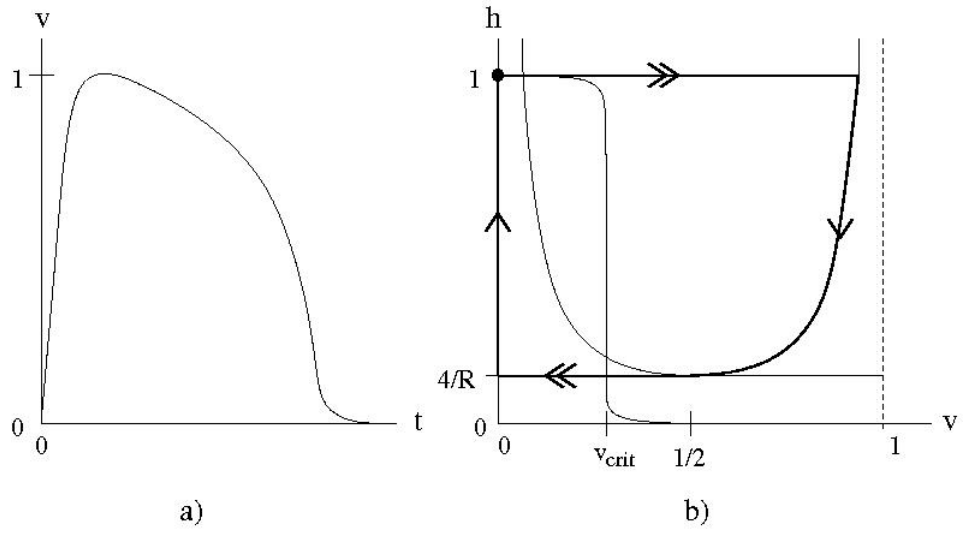

Figure 1: *a) A sketch of the v component of the pulse. b) A sketch of the nullclines associated with equation (1.7) and the leading order traveling pulse solution (bold) of equation (2.1).*

As mentioned above, this model has many similarities with the Fitzhugh-Nagumo equation, which was analyzed in [JKL91] and [Jon84] using geometric singular perturbation theory [Fen71, Fen79, Jon94, Kap99]. The above model also contains a small parameter, ϵ, indicating the presence of two separated time-scales on which the dynamics occur, and so we will use similar techniques in our analysis. On the other hand, there are key structural differences manifested predominantly in the inward current term $Rhv^2(1-v)$, which will lead to properties of the associated travelling pulse solution that are distinct from those of the pulse solution to the FitzHugh-Nagumo model. We will point to these differences throughout the paper.

If we consider the ODE associated with spatially independent solutions,

$$\begin{aligned} v_t &= Rhv^2(1-v) - v \\ h_t &= \epsilon g(v,h), \end{aligned}$$

we see that the v- and h-nullclines are given by the sets $\{v=0\} \cup \{h = 1/(Rv(1-v))\}$ and $\{g(v,h)=0\}$, respectively (see figure 1b). This provides intuition for the stationary solutions that one can expect to exist for the PDE (1.7). For the construction of the pulse, the v-nullcline will correspond to the slow manifold. Thus, we expect that the pulse will consist of four pieces: a fast jump in $\{h=1\}$ from $v=0$ to $v=v^+$, on the right branch of the v nullcline, a slow decay on the rightmost branch of the v-nullcline, a second fast jump in $\{h=4/R\}$ from $v=1/2$ to $v=0$, and a slow growth along the leftmost branch of the v-nullcline, back to the point $(v,h)=(0,1)$. We will assume that $R>4$, which is in accordance with our earlier comment on the size of the ratio τ_{out}/τ_{in} and their relative sizes in equation (1.3).

The key difference between this pulse and that of the FitzHugh-Nagumo model will be that the second 'fast' jump, in the present case, occurs at the knee of the v-nullcline. This point is exactly where the slow manifold of the singularly perturbed system loses normal hyperbolicity. As a direct consequence, the repolarization period of the wave back is much longer than the fast depolarization period of the wave front. (This explains the quotes in *the second 'fast' jump*, above.) This is one of the key features of membrane potentials in cardiac tissue.

The outline of the paper is as follows. Section 2 contains the proof of existence of traveling pulses. Section 3 is devoted to the stability analysis of such solutions. Finally, in section 4, we briefly discuss spatially

periodic traveling pulses, corresponding to successive heartbeats.

2 Existence of the Traveling Pulse

The main result of this section is Theorem 2.1, in which we prove that a traveling pulse, connecting $(v, h) = (0, 1)$ at $\xi = \pm\infty$, exists for all $\epsilon \in (0, \epsilon_0)$, where ϵ_0 is sufficiently small.

2.1 Construction of the pulse: $\epsilon = 0$

The traveling pulse is a stationary solution to the PDE (1.7) and also a solution to the ODE

$$\begin{aligned} v_\xi &= w \\ w_\xi &= cw - Rhv^2(1-v) + v \\ h_\xi &= \frac{\epsilon}{c} g(v, h). \end{aligned} \tag{2.1}$$

Notice that v and w are fast variables, while h is a slow variable. By setting $\epsilon = 0$ in the above system, we obtain the reduced fast system:

$$\begin{aligned} v_\xi &= w \\ w_\xi &= cw - Rhv^2(1-v) + v \\ h_\xi &= 0. \end{aligned} \tag{2.2}$$

By defining $y = \epsilon\xi$ in equation (2.1) and setting $\epsilon = 0$, we obtain the reduced slow system:

$$\begin{aligned} 0 &= w \\ 0 &= cw - Rhv^2(1-v) + v \\ h_y &= \frac{1}{c} g(v, h). \end{aligned} \tag{2.3}$$

First, consider the reduced slow equation (2.3). The associated leading order slow manifold is given by two pieces:

$$S_l = \{v = w = 0\}, \text{ and } \quad \tilde{S}_r = \{w = 0, h = \frac{1}{Rv(1-v)}\}.$$

We will be interested in S_l and the right branch of $\tilde{S}_r$, given by

$$S_r = \{w = 0, h = \frac{1}{Rv(1-v)}, v \geq \frac{1}{2}\}.$$

The slow dynamics on these manifolds are given by

$$\begin{aligned} h_y &= \frac{1}{c}(1-h) \quad \text{if} \quad (v, w) \in S_l \\ h_y &= -\frac{1}{c} h \qquad \text{if} \quad (v, w) \in S_r \end{aligned}$$

Next, consider system (2.2), where, due to the third equation, we may think of h as being a fixed parameter. For $1 \geq h > 4/R$, this equation has three fixed points: $(0, 0)$, $(v^+(h), 0)$, and $(v^-(h), 0)$, where

$$v^\pm(h) = \frac{1}{2} \pm \frac{1}{2}\sqrt{1 - \frac{4}{Rh}}. \tag{2.4}$$

Note that $(0,0) \in S_l$ and $(v^+(h),0) \in S_r$. In addition, this system is equivalent to the traveling wave equation associated with the PDE

$$v_t = v_{\xi\xi} - cv_\xi - Rhv(v - v^+(h))(v - v^-(h)). \tag{2.5}$$

In other words, system (2.2) is the ODE satisfied by stationary solutions of equation (2.5). Using the change of coordinates $v \to v^+(h)v$, $\xi \to (1/v^+(h)\sqrt{Rh})\xi$, $c \to -(v^+(h)\sqrt{Rh})c$, and $t \to t/[(v^+(h))^2 Rh]$, we see that this equation is just the bistable equation

$$v_t = v_{\xi\xi} + cv_\xi + v(1-v)(v-\mu).$$

In the above equation, $\mu = v^-(h)/v^+(h)$. Traveling wave solutions to the bistable equation are relatively well understood. See, for example, [Xin00]. In particular, for $0 < \mu < 1/2$, there is an exact formula for the unique traveling wave connecting $v = 0$ at $\xi = -\infty$ to $v = 1$ at $\xi = +\infty$. Similarly, for $1/2 < \mu < 1$, there is an exact formula for the unique wave connecting $v = 1$ at $\xi = -\infty$ to $v = 0$ at $\xi = +\infty$. Translating back to the original variables, we obtain the following formulae for the traveling wave solutions of the reduced fast equation:

$$v(\xi) = \frac{v^+(h)}{1 + e^{-\sqrt{\frac{Rh}{2}}v^+(h)\xi}}; \quad c = \sqrt{2Rh}\left(\frac{1}{2}v^+(h) - v^-(h)\right) \text{ if } \quad \frac{1}{2}v^+(h) - v^-(h) > 0, \tag{2.6}$$

and

$$v(\xi) = \frac{v^+(h)}{1 + e^{\sqrt{\frac{Rh}{2}}v^+(h)\xi}}; \quad c = -\sqrt{2Rh}\left(\frac{1}{2}v^+(h) - v^-(h)\right) \text{ if } \quad \frac{1}{2}v^+(h) - v^-(h) < 0. \tag{2.7}$$

Notice this implies that, if $\frac{1}{2}v^+(h) - v^-(h) > 0$, then there is a unique heteroclinic connection between $v = 0$ at $-\infty$ and $v = v^+(h)$ at $+\infty$ (see figure 3a). When $\frac{1}{2}v^+(h) - v^-(h) < 0$, then there is a unique connection going in the opposite direction. Using the formulas for $v^\pm(h)$, given in equation (2.4), one can see that the value of h for which $\frac{1}{2}v^+(h) - v^-(h) = 0$ is given by $\bar{h} = \frac{9}{2R}$.

It may be of interest to note the following. If one considers equation (2.5) with $c = 0$, then the associated ODE is Hamiltonian with $H(v, v') = (v')^2/2 - v^2/2 + Rhv^3/3 - Rhv^4/4$, where $v' = v_\xi$. For positive wavespeeds $c > 0$, $dH/d\xi = c(v')^2$. As h decreases through $\bar{h}$, the value of $H(v^+(h), 0)$ switches from being positive to negative. As a result, for $h > \bar{h}$, there is no way to have a connection going from $v = v^+(h)$ to $v = 0$, and, for $h < \bar{h}$, there is no way to go in the opposite direction.

The above reduced fast analysis was for $h \in (4/R, 1]$. If $h = 4/R$, however, we have $v^+(h) = v^-(h)$, and the structure of the reduced fast system changes. In that case, equation (2.2) becomes

$$\begin{aligned} v_\xi &= w \\ w_\xi &= cw + v(2v-1)^2 \end{aligned}$$

which is equivalent to the traveling wave equation for the PDE

$$v_t = v_{\xi\xi} - cv_\xi - v(2v-1)^2. \tag{2.8}$$

Up to a change of variables, this PDE is exactly the generalized Fisher-KPP equation of order 2 [Xin00]. For each $c \geq \sqrt{2}/2$, equation (2.8) has a heteroclinic orbit connecting $(1/2, 0)$ at $-\infty$ with $(0,0)$ at $+\infty$. If $c > \sqrt{2}/2$, then the orbit leaves $(1/2, 0)$ along a center manifold and approaches $(0,0)$ along its stable manifold (see figure 3b). If $c = \sqrt{2}/2$, known as the critical wavespeed, then the orbit leaves $(1/2, 0)$ along

the unstable manifold and approaches $(0,0)$ along its stable manifold. For more information on critical wavespeeds in this and other related equations, see, for example, [PK06].

Putting the information from the reduced slow and fast dynamics together, we expect that the leading order pulse will consist of four pieces:

1. A fast jump from $(0,0,1)$ to $(v^+(1),0,1)$, which is given explicitly in equation (2.6), with $c^* = c(R,1)$;
2. Slow decay along S_r to a point $(v^+(h^*),0,h^*)$, where h^* will be determined by the third piece of the pulse.
3. A fast jump from $(v^+(h^*),0,h^*)$ to $(0,0,h^*)$, at the value of $h^* \in [4/R,1)$ such that $c^* = c^*(R,h^*)$; and
4. Slow growth along S_l back to $(0,0,1)$.

Notice that the first piece will determine the wavespeed $c^* = c(R,1)$. The value of h^* at which the third piece occurs will be determined by the relation in equation (2.7) and will be the value of $h \in [4/R,1)$ such that $c(R,1) = c^* = c(R,h^*)$. A sketch of the function $c(R,h)$, for fixed R, is given in figure 2.

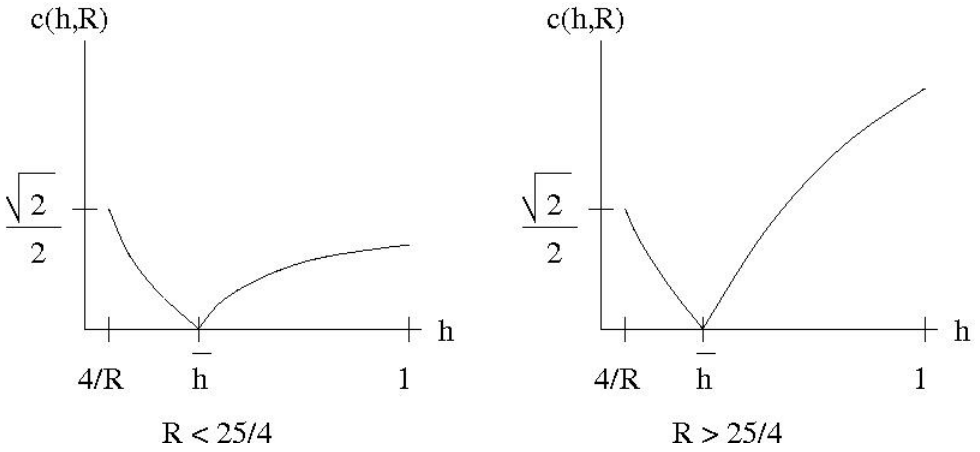

Figure 2: *A sketch of the function $c(R,h)$, as given in equations (2.6) and (2.7), for fixed R.*

If $0 < R < 25/4$, then there exists an $h^* \in (4/R, \bar{h})$ for which the reduced fast system (2.2) has a heteroclinic orbit of speed c^* connecting $(v+(h^*),0)$ at $-\infty$ with $(0,0)$ at $+\infty$. However, if $R > 25/4$, there is no such $h^* \in (4/R, \bar{h})$.

Recall that, based upon the relative sizes in equation (1.2), we expect R to be large. As a result, we are interested in the case where $R > 25/4$. Thus, the second fast jump must occur for $h = 4/R$, because for this value of h a connection exists for all $c \geq \sqrt{2}/2$. As a result, the complete, leading order pulse is given by a curve as sketched in figure 4.

This situation corresponds to the pulse leaving the slow manifold at the knee, which is exactly the point where the manifold ceases to be normally hyperbolic. Therefore, it is not immediately clear what will happen to the pulse for $\epsilon > 0$. Furthermore, because $c(R,1) > \sqrt{2}/2$ (for $R > 25/4$), the second fast jump leaves the knee along the center, rather than the unstable, manifold. This will create a slow transition between the first slow and second fast piece of the pulse, due to the algebraic, rather than exponential, growth away from the slow manifold in the singular limit.

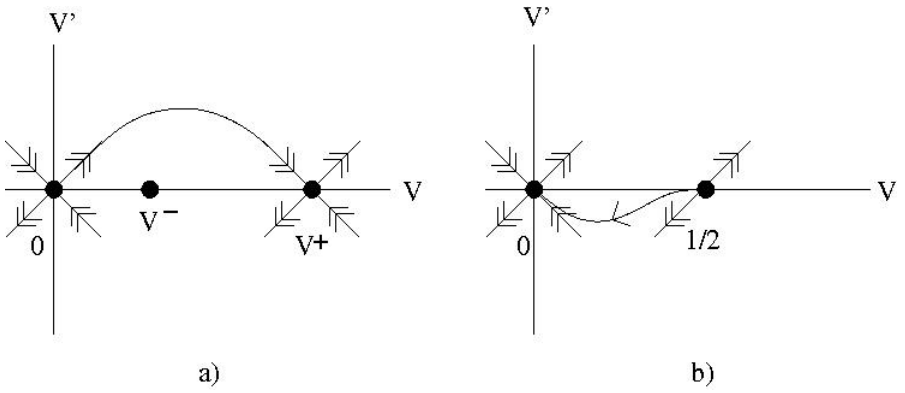

Figure 3: *A sketch of the phase planes for the leading order fast components of the pulse: a) the traveling pulse of equation (2.5), for* $\frac{1}{2}v^+ - v^- > 0$*; b) the traveling pulse of equation (2.8), for* $c > \sqrt{2}/2$*, which is asymptotic to the center manifold at* $-\infty$*.*

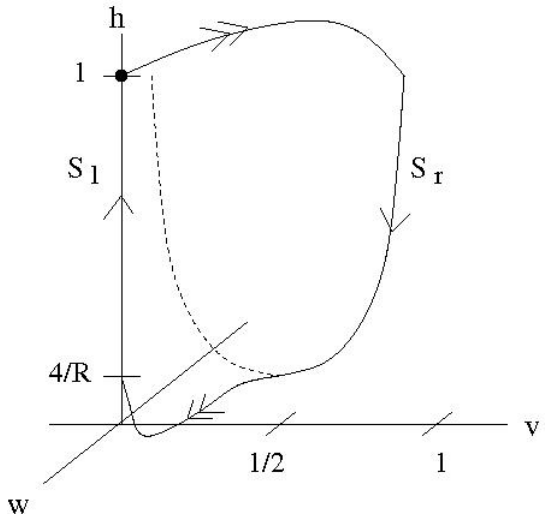

Figure 4: *A sketch of the leading order pulse, consisting of a fast jump from* $(0,0,1)$ *to* $(v^+(1),0,1)$*, slow decay along* S_r*, another fast jump connecting* $(1/2,0,4/R)$ *to* $(0,0,4/R)$ *and leaving at the knee, and slow growth along* S_l*.*

2.2 Persistence of the pulse: $1 \gg \epsilon > 0$

The above analysis tells us what the pulse looks like, to leading order. In order to show that a traveling pulse exists for $0 < \epsilon \ll 1$, we will track the leading-order center-unstable manifold of $(0,0,1)$, which we will denote by W^{cu}, forwards along the first fast jump, down the slow manifold, and along the second fast jump. In addition, we will track the leading-order center-stable manifold of $(0,0,1)$, denoted by W^{cs}, backwards down along the left-most piece of the slow manifold. We will show that, for $\epsilon = 0$, these manifolds intersect transversely, which proves that a traveling pulse must also exist for ϵ positive and sufficiently small.

There are two main difficulties in tracking the center-unstable manifold W^{cu} along the pulse. The first difficulty lies in following W^{cu} along the slow manifold S_r for large times. However, there is a tool, known as the Exchange Lemma and proved in [JK94], which will allow us to do this. Second, complications can arise due to the lack of normal hyperbolicity at the knee. Analysis in a neighborhood of the knee can be carried out using a geometric desingularization technique known as blow-up [KS01]. Using these

techniques, we will prove the following theorem.

Theorem 2.1. *Let ϕ_0 denote the formal traveling pulse solution of equation (1.5) for $\epsilon = 0$, constructed in section 2.1. More specifically, ϕ_0 is defined by the union of the following curves in the (v, v_ξ, h) phase space. Define $S_l = \{v = v_\xi = 0, h \in [4/R, 1]\}$, $S_r = \{v \in [1/2, v^+(1)], v_\xi = 0, h = \frac{1}{Rv(1-v)}\}$, $F_F = \{(v, v_\xi)$ given by (2.6) for $\xi \in \mathbb{R}, h = 1\}$, and $F_B = \{(v, v_\xi)$ the traveling wave solution of (2.8) when $c = c^* > \sqrt{2}/2$ for $\xi \in \mathbb{R}, h = 4/R\}$. Then*

$$\phi_0 = F_F \cup S_r \cup F_B \cup S_l.$$

If $\epsilon_0 > 0$ is sufficiently small, then for all $\epsilon \in (0, \epsilon_0)$ there exists a traveling pulse solution of equation (1.5), $\phi_\epsilon(\xi) = (V(\xi;\epsilon), V_\xi(\xi,\epsilon), H(\xi;\epsilon))$, satisfying

$$\lim_{\xi \to \pm\infty} (V(\xi;\epsilon), V_\xi(\xi,\epsilon), H(\xi;\epsilon)) = (0, 0, 1),$$

and lying as a curve within $\mathcal{O}(\epsilon^{2/3})$ of the set ϕ_0.

Remark 2.2. *In the statement of the above theorem, the perturbed pulse is parameterized by the spatial variable ξ. The leading order pulse, ϕ_0, can not be parameterized in this way. This is because, for $\epsilon = 0$, it takes an infinite amount of "time" for the pulse to traverse each piece of the leading order orbit in the phase space. This is why the leading order pulse is defined geometrically, in terms of the sets F_F, S_r, F_B, S_l.*

Proof: First, we remark that, along various pieces of the leading-order pulse, different quantities (ie v, w, h, c, ϵ) will determine the key properties of the tracked manifold. Thus, we will consider only the relevant equations for $v_\xi, w_\xi, h_\xi, c_\xi$, or ϵ_ξ along each of the two fast and two slow components of the pulse. With a slight abuse of notation, we will still refer to the tracked manifold as the center-stable or center-unstable manifold along each piece and hope that it will be clear from the context exactly which variables we are keeping track of at the time.

We begin by tracking W^{cu} along the first fast jump. Consider the reduced fast system, equation (2.2). The plane $\{h = 1\}$ is invariant, and we want to determine how the unstable manifold of $(v, w) = (0, 0)$ intersects the stable manifold of $(v, w) = v^+(1), 0)$ as we vary the wavespeed c. To do this, we fix $h = 1$ and append to (2.2) the equation $c_\xi = 0$:

$$\begin{aligned} v_\xi &= w \\ w_\xi &= cw - Rv^2(1-v) + v \\ c_\xi &= 0. \end{aligned} \tag{2.9}$$

Based upon the analysis of the bistable equation, mentioned above, there is a unique $c^* = c^*(R)$ for which a unique heteroclinic connection between the saddle $(0, 0)$ at $-\infty$ and the saddle $(v^+(1), 0)$ at $+\infty$ exists. We will show that the two-dimensional center-unstable manifold, which is a union of the unstable manifolds of $(v, w) = (0, 0)$ for values of c near c^* and denoted by $W^{cu}(0, 0)$, intersects the two-dimensional center-stable manifold of $(v^+(1), 0)$ (again defined as a union of the stable manifolds for c near c^*), denoted by $W^{cs}(v^+(1), 0)$, and that this intersection is transverse in the c direction. In other words, upon varying c along the fibers within the center-unstable and center-stable manifolds, there is an intersection for a unique value, $c = c^*$, and the manifolds intersect transversely at this point.

One way to track the evolution of two-dimensional manifolds is using two-forms, as in [JKL91]. This essentially allows one to track the evolution of their tangent planes. The vector of one-forms associated

with equation (2.9) is (dv, dw, dc), and its evolution is given by

$$\begin{aligned} dv' &= dw \\ dw' &= \left(1 - R2v(1-v) + Rv^2\right) dv + cdw + wdc \\ dc' &= 0, \end{aligned}$$

where $(\cdot)' = d/d\xi$. The associated two-forms are $P_{vw} = dv \wedge dw$, $P_{vc} = dv \wedge dc$, and $P_{wc} = dw \wedge dc$, with evolution equations

$$\begin{aligned} P'_{vw} &= cP_{vw} + wP_{vc} \\ P'_{vc} &= P_{wc} \\ P'_{wc} &= \left(1 - R2v(1-v) + Rv^2\right) P_{vc} + cP_{wc}. \end{aligned}$$

These equations can be analyzed as in [JKL91], and we restate the details here for convenience. To be precise, we really should think of $\{P_{vw}, P_{vc}, P_{wc}\}$ as the basis for the space of two-forms in vwc-space and write an arbitrary element as $f_1(v,w,c)P_{vw} + f_2(v,w,c)P_{vc} + f_3(v,w,c)P_{wc}$. It is really the coefficients f_i that we want to determine. The notation in the above system is therefore an abuse of notation: $P_{vw}(\xi)$ denotes the coefficient $f_1(v,w,c)(\xi)$, and so on. As this notation has become somewhat standard (for example, in system (2.1) we are in some sense thinking of $\{v, w, h\}$ as a basis for $\mathbb{R}^3$, particularly when we plot the phase diagram in figure (4)), we use it in the following.

Consider the equation for P_{vw}, and let $P^{\pm}_{vw}$ and $P^{\pm}_{vc}$ be the two forms associated with manifolds $W^{cu}(0,0)$ ($-$, coming from $-\infty$) and $W^{cs}(v^+(1),0)$ ($+$, coming from $+\infty$). We will show that P^+_{vc} and P^+_{vw} have the same sign, whereas P^-_{vc} and P^-_{vw} have the opposite sign. This implies that the vectors of two-forms associated with the manifolds, $(P^{\pm}_{vw}, P^{\pm}_{vc}, P^{\pm}_{wc})$, are linearly independent and, hence, that the manifolds intersect transversely.

The manifolds $W^{cu}(0,0)$ and $W^{cs}(v^+(1),0)$ both have the vector field, $(w, cw - Rv^2(1-v) + v, 0)$, as one tangent vector. Denote the other one by $(dv^{\pm}, dw^{\pm}, 1)$, respectively, where we can take $dc = 1$ since $dc' = 0$. This ensures the two tangent vectors for each manifold are linearly independent. The two-forms for each tangent plane are, up to a positive normalization factor N, given by 2×2 subdeterminants of a 2×3 matrix, whose rows are exactly the above tangent vectors. Thus, we have

$$P^{\pm}_{vc} = N \det \begin{pmatrix} w & 0 \\ dv^{\pm} & 1 \end{pmatrix} = Nw.$$

As a result, the equation for P_{vw} is given by

$$P'_{vw} = cP_{vw} + Nw^2.$$

Since both $W^{cu}(0,0)$ and $W^{cs}(v^+(1),0)$ asymptotically contain a line of fixed points in the c-direction, we know that $P^+_{vw} \to 0$ as $\xi \to +\infty$, and $P^-_{vw} \to 0$ as $\xi \to -\infty$. Using the above equation, we can then see that $P^-_{vw} > 0$ and $P^+_{vw} < 0$ along the manifolds. Since $P^{\pm}_{vc} = Nw$ and w is positive along the first fast jump, $P^{\pm}_{vc} > 0$. Thus, the manifolds intersect transversely.

In order to continue tracking W^{cu} along the slow manifold S_r, we will need to use the Exchange Lemma [JK94]. This lemma tells us how information in the center direction, corresponding to the wavespeed c, at the top of S_r is exchanged for information in the center direction, corresponding to h, at the bottom of S_r. More specifically, the lemma tells us that, since W^{cu} is transverse to $W^{cs}(v^+(1),0)$, when it leaves a

neighborhood of S_r near any point with $1 > h > 4/R$, the tangent plane to W_{cu} will be C^1 $\mathcal{O}(\epsilon)$ close to the plane spanned by the tangent line to S_r in the plane $\{w = 0\}$ and the fast unstable fiber of the point $(v^+(h), 0, h)$. Thus, at a given value of h, the tangent plane to W^{cu} will be spanned, to leading order, by the vectors

$$\left(1, 0, \frac{2v^+(h) - 1}{2(v^+(h))^2(1 - v^+(h))^2}\right), \quad \left(1, \frac{c}{2} + \frac{\sqrt{c^2 + 4(Rhv^+(h) - 2)}}{2}, 0\right). \tag{2.10}$$

The exchange lemma tells us what W^{cu} looks like up to a neighborhood of the knee, when $h = 4/R$. At this point, the slow manifold S_r is not normally hyperbolic, and so we'll need to use blow-up to track the manifold around the knee.

2.2.1 Analysis of the Knee

Consider the ODE for the pulse, equation (2.1), and append to it an equation for ϵ:

$$\begin{aligned} v_\xi &= w \\ w_\xi &= cw - Rhv^2(1 - v) + v \\ h_\xi &= \frac{\epsilon}{c} g(v, h) \\ \epsilon_\xi &= 0. \end{aligned} \tag{2.11}$$

Because the first fast jump selected the wavespeed $c = c(\epsilon)$, where $c(0) = c^*$, we now think of c as being fixed. (For notational convenience we do not explicitly write the epsilon dependence.) The relevant center directions, therefore, are now given by h, and also by ϵ.

We are interested in the behavior of this equation near the knee, which corresponds to the fixed point $(1/2, 0, 4/R, 0)$. The Jacobian at this point is given by

$$J = \begin{pmatrix} 0 & 1 & 0 & 0 \\ 0 & c & -R/8 & 0 \\ 0 & 0 & 0 & -4/(cR) \\ 0 & 0 & 0 & 0 \end{pmatrix}.$$

This matrix has one positive eigenvalue, $\lambda = c$, with associated eigenvector $(1, c, 0, 0)$. In addition, $\lambda = 0$ is an eigenvalue with algebraic multiplicity three and geometric multiplicity one. The associated eigenvector is $(1, 0, 0, 0)$, and the generalized eigenvectors are $(0, 1, 8c/R, 0)$ and $(0, 0, -8/R, -2c^2)$. In order to do the blow-up, we will need to isolate the nonhyperbolic dynamics, which occur on a three-dimensional center manifold. In a neighborhood of the knee, this manifold can be represented by

$$\begin{aligned} w &= F\left((v - 1/2), (h - 4/R), \epsilon\right) \\ &= \alpha_0(h - 4/R) + \alpha_1\epsilon + \beta_0(v - 1/2)^2 + \beta_1(h - 4/R)^2 + \beta_2\epsilon^2 \\ &\quad + \gamma_0(v - 1/2)(h - 4/R) + \gamma_1(v - 1/2)\epsilon + \gamma_2(h - 4/R)\epsilon + \mathcal{O}(3), \end{aligned} \tag{2.12}$$

where α_i, β_i, and γ_i are constants. We remark that the center manifold is not unique. However, the analysis that we carry out below is valid up to exponentially small terms, and thus is independent of the choice of the center manifold.

One can explicitly compute the above coefficients. As we will see below, the ones that will be relevant for the blow-up analysis are:

$$\alpha_0 = R/(8c), \quad \beta_0 = -2/c.$$

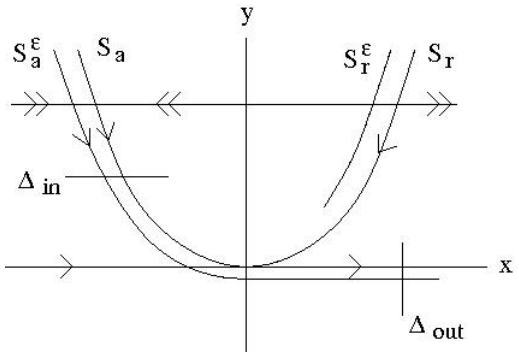

Figure 5: *A sketch of the slow manifolds and sections for the fold, as analyzed in [KS01].*

Inserting these into equation (2.11), one sees that the dynamics on the center manifold are given by

$$\begin{aligned} v_\xi &= -\frac{2}{c}(v-\frac{1}{2})^2 + \frac{R}{8c}(h-\frac{4}{R}) + \mathcal{O}\left(\epsilon, (h-\frac{4}{R})^2, \epsilon^2, (v-\frac{1}{2})(h-\frac{4}{R}), \epsilon(h-\frac{4}{R}), \epsilon(v-\frac{1}{2})\right) \\ h_\xi &= -\frac{4}{Rc}\epsilon + \mathcal{O}(\epsilon(h-\frac{4}{R})) \\ \epsilon_\xi &= 0. \end{aligned} \tag{2.13}$$

This system is essentially the normal form for a fold point, given in [KS01]. Their analysis explains why the terms of order $\mathcal{O}\left(\epsilon, (h-\frac{4}{R})^2, \epsilon^2, (v-\frac{1}{2})(h-\frac{4}{R}), \epsilon(h-\frac{4}{R}), \epsilon(v-\frac{1}{2})\right)$ are all indeed higher order. We now collect the results from [KS01] that are relevant for this paper.

In [KS01], the authors analyze systems of the form

$$\begin{aligned} x' &= -y + x^2 + \mathcal{O}(\epsilon, xy, y^2, x^3) \\ y' &= -\epsilon + \mathcal{O}(\epsilon x, \epsilon y, \epsilon^2). \end{aligned} \tag{2.14}$$

This system possesses a slow manifold that, for $\epsilon = 0$, is given by $S = \{(x,y) : y = x^2\}$. It can be divided into the attracting and repelling branches of the parabola, denoted by S_a and S_r, respectively. (To be consistent with the notation in [KS01], we use S_r to denote the repelling branch and hope that it will not be confused with the right branch of the slow manifold, given in equation (2.1).) Outside a neighborhood of the fold point, $(0,0)$, these manifolds are normally hyperbolic and, therefore, perturb smoothly to locally invariant manifolds S_a^ϵ and S_r^ϵ, for ϵ positive and sufficiently small (see figure 5).

Their main result describes what happens in a neighborhood of $(0,0)$ for $0 < \epsilon \ll 1$, and it can be explained as follows. Let $\Delta_{in} = \{(x, \rho^2), x \in I\}$ and $\Delta_{out} = \{(\rho, y), y \in \mathbb{R}\}$, where $I \subset \mathbb{R}$ is a suitable interval. Let $\pi : \Delta_{in} \to \Delta_{out}$ be the transition map associated with the flow of (2.14) (see figure 5).

Proposition 2.3. *[KS01] There exists an $\epsilon_0 > 0$ such that, for $\epsilon \in (0, \epsilon_0)$,*

1. *The manifold S_a^ϵ passes through Δ_{out} at a point $(\rho, y(\epsilon))$, where $y(\epsilon) = \mathcal{O}(\epsilon^{2/3})$. In particular, $y(\epsilon) = -\Omega_0 \epsilon^{2/3} + o(\epsilon^{2/3})$, where $\Omega_0 > 0$ is known explicitly.*
2. *The transition map π is a contraction with contraction rate $\mathcal{O}(e^{-k/\epsilon})$, where k is a positive constant.*

The first item of this proposition tells us how to track the manifold W^{cu} around the knee. The second tells us that the resulting analysis will be independent of the choice of center manifold. We note the scaling $\epsilon^{2/3}$ is consistent with the higher order asymptotics of the restitution curve, computed in [MS03, CS06].

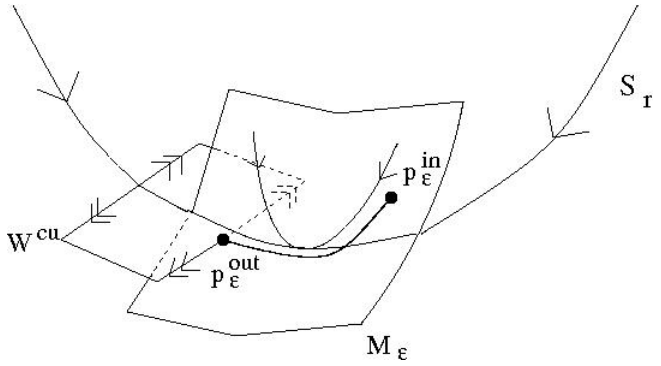

Figure 6: *A schematic diagram, in a neighborhood of the knee, of the tracked manifold W^{cu}. It is guided by the trajectory through the points p_ϵ^{in} and p_ϵ^{out}, which lies on the center manifold M_ϵ.*

As mentioned above, for any $h \in (4/R, 1)$, the two-dimensional manifold W^{cu} is spanned by the one-dimensional fast unstable direction of the points $(v, w) = (v^+(h), 0)$ and the tangent line in the plane $\{w = 0\}$ to the one dimensional slow manifold, given by $h = 1/(Rv(1-v))$. As W^{cu} enters a neighborhood of the knee, it will intersect the center manifold of the knee, given in equation (2.12). We will denote this center manifold by $M_\epsilon = \{w = F(v, h, \epsilon)\}$ and its leading order version by $M_0 = \{w = F(v, h, 0)\}$.

In order to see how the dynamics on center manifold at the knee will guide W^{cu}, define the following objects (with a slight abuse of notation, we will reuse the quantities $\Delta_{in,out}$ and ρ from the fold analysis):

$$\begin{aligned}
\Delta_{in} &= \{(v, w, h) : h = \frac{4}{R} + \rho^2\} \\
\Delta_{out} &= \{(v, w, h) : v = \frac{1}{2} - \rho\} \\
I^{u,in} &= W^{cu} \cap \Delta_{in} \\
p_\epsilon^{in} &= I^{u,in} \cap M_\epsilon \\
I^{u,out} &= W^{cu} \cap \Delta_{out} \\
p_\epsilon^{out} &= I^{u,out} \cap M_\epsilon
\end{aligned}$$

Both Δ_{in} and Δ_{out} are two-dimensional objects, as is W^{cu}. $I^{u,in}$ and $I^{u,out}$, however, are one-dimensional, and $p_\epsilon^{in,out}$ are points (at least for fixed ϵ, when M_ϵ is two-dimensional).

Because the point p_ϵ^{in} lies on the center manifold M_ϵ, its evolution will be governed by the dynamics of the fold. The trajectory through p_ϵ^{in} will follow the attracting critical manifold S_a^ϵ around the knee, and exit the neighborhood of the knee on the section Δ_{out} at the point p_ϵ^{out}. Since p_ϵ^{in} is also in W^{cu}, the tracked manifold will follow its trajectory around the knee. Upon exiting a neighborhood of the knee, W^{cu} will be spanned by the one-dimensional direction of the flow at p_ϵ^{out}, and the one-dimensional fast fibers of M_ϵ at p_ϵ^{out}. See figure 6.

The important information to take away from the analysis at the knee is the following. When $\epsilon = 0$, the manifold W^{cu} is tangent at the knee to the plane spanned by the vectors $(1, 0, 0)$ and $(1, c, 0)$, which are obtained by setting $v = 1/2$ in equation (2.10), and has height $h = 4/R$. We need to know how this picture changes for ϵ positive and small. Based on the above analysis, we see that, on leaving a neighborhood of the knee, the tangent plane to W^{cu} is spanned by a vector tangent to the fast unstable fibers of M_ϵ and a vector in the direction of the flow. We know that the unstable fibers of the center manifold M_ϵ perturb smoothly, so their h component will be $\mathcal{O}(\epsilon)$. The other tangent vector is given by the flow, whose

h component is $\mathcal{O}(\epsilon)$. In addition, the height of the tangent plane to W^{cu} is given by $h = 4/R - \mathcal{O}(\epsilon^{2/3})$. Therefore, upon leaving a neighborhood of the knee, the perturbed manifold W^{cu} will be $\mathcal{C}^1$ $\mathcal{O}(\epsilon^{2/3})$ close to the unperturbed one. We remark that the C^1 aspect of the perturbation follows from the fact that the center manifold itself is normally hyperbolic, and therefore its unstable fibers perturb smoothly. It is these fibers that make up W^{cu}. Proposition 2.3 then ensures that the base points of these fibers can change by no more than $\mathcal{O}(\epsilon^{2/3})$.

2.2.2 Completion of the existence proof

We will now follow W^{cu} along the back and W^{cs} backwards down the left branch of the slow manifold and show they intersect transversely. This will complete the existence argument.

We have shown above that when W^{cu} leaves a neighborhood of the knee, its tangent plane is close to a plane that is parallel to the vw plane. One can see directly from equation (2.1) that, to leading order, any plane parallel to the vw plane is invariant. There is only a finite amount of time between when W^{cu} leaves a neighborhood of the knee and when it enters a neighborhood of the point $(0, 0, 4/R)$. Therefore, by choosing ϵ sufficiently small, we can make the tangent plane to W^{cu}, upon entering this neighborhood, as close to a plane parallel to the vw plane as we like.

The center stable manifold of $(0, 0, 1)$, W^{cs}, consists of the union of the stable manifolds of the saddle points $(0, 0)$ for $h \in [4/R, 1]$. As a result, it will transversely intersect any plane which is parallel to the vw plane. This implies that W^{cs} intersects W^{cu} transversely, which completes the proof. □

3 Stability of the pulse

The goal of this section will be to prove the following theorem on the linear stability of the traveling pulse.

Theorem 3.1. *The traveling pulse solution, constructed in section 2, is spectrally stable. In other words, the operator obtained by linearizing around the wave (see equation (3.1)) has no spectrum in* $\{\mathrm{Re}(\lambda) \geq 0\}$ *except for an isolated eigenvalue at the origin of geometric and algebraic multiplicity one.*

We remark that linear stability of the wave follows from a spectral mapping theorem for the strongly continuous semigroup generated by the linear operator in equation (3.1). In addition, because the zero eigenvalue is isolated, standard arguments, such as invariant manifold theory, can be used to show that the traveling pulse is nonlinearly stable, as well [BJ89].

The outline of the proof is as follows. First, we will show that the essential spectrum is bounded to the left of the imaginary axis – although the bound will be dependent on ϵ. We will then construct the Evans function [Eva73, AGJ90] associated with the full problem, for $\epsilon > 0$, followed by the Evans functions associated with the reduced fast pieces along the front and back of the pulse. This will be done in section 3.1. We will then show that eigenvalues of the full Evans function are determined by those of the reduced problems, and use information about the stability of the pulses in the bistable and generalized KPP equations to determine the stability of the pulse. This will be done in section 3.2.

There are two key elements of the argument. First, the spectrum of the reduced fast problem along the back, corresponding to the generalized KPP equation, contains essential spectrum that accumulates at the origin. Thus, one must be careful in analyzing the associated reduced Evans function. We will appeal to

the results of [WXY06], in which the Evans function for algebraically decaying solutions to such equations was analyzed. Second, the loss of normal hyperbolicity at the knee could potentially allow the zeros of the full Evans function to be different than those of the reduced problem. Using techniques similar to those of the existence argument, above, we will see that this is not the case.

3.1 Essential spectrum and definition of the Evans function

We will denote the persistent traveling pulse solution to equation (1.7) by $(V(\xi), H(\xi))$. (Note that this solution is also dependent on the parameter ϵ, although we will surpress this in our notation.) In order to consider the stability of the pulse, assume that solutions to equation (1.7) have the form $(v,h)(\xi,t) = (V(\xi),H(\xi)) + (p,r)(\xi,t)$. The linearized flow for the new coordinates (p,r), which represent the perturbation of the wave, is then given by

$$\begin{aligned} p_t &= p_{\xi\xi} - cp_\xi + \left(2RHV(1-V) - RHV^2 - 1\right)p + RV^2(1-V)r \\ r_t &= -cr_\xi + \epsilon g_v(V,H)p - \epsilon r. \end{aligned} \tag{3.1}$$

The associated eigenvalue problem, when written as a first order system, is given by

$$\begin{aligned} p_\xi &= q \\ q_\xi &= \left(\lambda - 2RHV(1-V) + RHV^2 + 1\right)p + cq - RV^2(1-V)r \\ r_\xi &= \epsilon\frac{g_v(V,H)}{c}p - \frac{(\lambda+\epsilon)}{c}r. \end{aligned} \tag{3.2}$$

We can write this eigenvalue problem using matrix notation

$$\frac{d}{d\xi}\begin{pmatrix} p \\ q \\ r \end{pmatrix} = A(\xi,\lambda)\begin{pmatrix} p \\ q \\ r \end{pmatrix}, \tag{3.3}$$

where

$$A(\xi,\lambda) = \begin{pmatrix} 0 & 1 & 0 \\ \lambda - 2RHV(1-V) + RHV^2 + 1 & c & -RV^2(1-V) \\ \epsilon\frac{g_v(V,H)}{c} & 0 & -\frac{(\lambda+\epsilon)}{c} \end{pmatrix}, \tag{3.4}$$

and the ξ dependence is through the underlying wave, $(V,H) = (V(\xi),H(\xi))$.

3.1.1 Location of the essential spectrum

The essential spectrum is determined by the asymptotic limits of the matrix A, defined in equation (3.4), which are given by

$$\begin{aligned} A^\infty(\lambda) &= \lim_{\xi\to\pm\infty} A(\xi,\lambda) \\ &= \begin{pmatrix} 0 & 1 & 0 \\ \lambda+1 & c & 0 \\ 0 & 0 & -\frac{(\lambda+\epsilon)}{c} \end{pmatrix}. \end{aligned} \tag{3.5}$$

The boundary of the essential spectrum is given by all values of λ for which this matrix has purely imaginary eigenvalues [Hen81]. This set is given by

$$\{-\epsilon - ick : k \in \mathbb{R}\} \cup \{-k^2 - ick - 1 : k \in \mathbb{R}\}.$$

In addition, by [Hen81], the essential spectrum lies to the left of the above boundary: $\sigma_{ess} \subset \{\lambda \in \mathbb{R} : \mathrm{Re}(\lambda) \leq -\epsilon\}$. In the limit $\epsilon \to 0$, the essential spectrum will approach the imaginary axis. However, this will not affect the definition of the Evans function, as given below. We define $\Omega = \Omega(\epsilon)$ to be the open region in the complex plane that lies to the right of the essential spectrum, containing the right half plane.

3.1.2 Definition of the Evans function

The eigenvalues of the asymptotic matrix $A^{\infty}(\lambda)$, defined in equation (3.5), are given by

$$\nu_0 = -\frac{(\lambda+\epsilon)}{c}, \quad \nu^{\pm} = \frac{c}{2} \pm \frac{1}{2}\sqrt{c^2 + 4(\lambda+1)},$$

For $\lambda \in \Omega$, $\nu^+(\lambda)$ is the unique eigenvalue with positive real part. One can check that there exists a b, independent of ϵ, such that, for all ϵ sufficiently small and all $\lambda \in \tilde{\Omega} := \{\lambda : \mathrm{Re}(\lambda) > -b\}$, $\nu^+(\lambda)$ remains the unique eigenvalue with largest real part. (Note that $\tilde{\Omega}$ is slightly large than, but contains, Ω, for ϵ sufficiently small.) This remains true even when the real part of ν_0 changes sign. The eigenvector associated with ν^+ is given by $X^+ = (1, \nu^+, 0)^t$. As a result, there exists a unique solution to equation (3.3), $\zeta(\xi, \lambda)$, such that

$$\lim_{\xi \to -\infty} \zeta(\xi, \lambda) e^{-\nu^+(\lambda)\xi} = X^+(\lambda). \tag{3.6}$$

Consider now the associated adjoint problem,

$$\frac{d}{d\xi} Z = -\bar{A}^T(\lambda, \xi) Z, \tag{3.7}$$

Similarly, for $\lambda \in \tilde{\Omega}$, there is a unique eigenvalue of the associated asymptotic matrix with smallest real part. This eigenvalue is given by $\mu^-(\lambda) = -\bar{\nu}^+(\lambda)$, and its associated eigenvector is $Y^- = (\mu^- - c, 1, 0)^t$. For $\lambda \in \tilde{\Omega}$, we have that $\mathrm{Re}(\mu^-) < 0$. There exists a unique solution to (3.7), $\eta(\xi, \lambda)$, such that

$$\lim_{\xi \to +\infty} \eta(\xi, \lambda) e^{-\mu^-(\lambda)\xi} = Y^-(\lambda). \tag{3.8}$$

The Evans function [AGJ90] is then defined by

$$D(\lambda) = \zeta(\xi, \lambda) \cdot \eta(\xi, \lambda). \tag{3.9}$$

As in [Jon84], $D(\lambda)$ can be shown to be analytic on $\tilde{\Omega}$. This is because ν^+ and μ^- are the unique eigenvalues with largest and smallest real part, respectively, in $\tilde{\Omega}$, uniformly in ϵ, even as λ crosses into the essential spectrum. (For addition information on the extension of the Evans function into the essential spectrum, see, for example, [KS98, GZ98].) For $\lambda \in \Omega$, the zeros of $D(\lambda)$, along with their multiplicities, correspond to the eigenfunctions of the linear operator in equation (3.1). For $\lambda \in \tilde{\Omega}$, however, this relationship does not necessarily hold. Technically, the actual Evans function, $D(\lambda)$, is only defined on Ω, and the Evans function we consider is an analytic extension of it (sometimes denoted by $\tilde{D}(\lambda)$) into $\tilde{\Omega}$. We will not emphasize this distinction here.

3.2 Locating zeros of $D(\lambda)$ in the right half plane

The goal of this section is to show that the only zero of $D(\lambda)$ with $\mathrm{Re}(\lambda) \geq 0$ is $\lambda = 0$, and that its geometric and algebraic multiplicity is one. The argument will be similar to that in [Jon84], although we

will have to do a bit of extra work to account for the loss of hyperbolicity in the knee of the existence construction.

The outline of the argument is as follows. First, we will construct the reduced Evans functions associated with the fast flow along the front and back of the pulse and show that the only zero in the closed right half plane is at the origin and associated with the front. The back does not contribute a zero there because of its algebraic decay at $-\infty$. This is a key difference between this problem and the stability of the pulse in FitzHugh-Nagumo. Next, it will be shown that any zeros of the full Evans function must be close to zeros of the reduced Evans functions. Thus, because there exists a unique zero of the reduced Evans functions in the right half plane, and we know it remains at zero for the full system due to translation invariance of the underlying wave, the wave must be spectrally stable. Note that it is not necessary to compute the derivative of the Evans function at the origin, as it was for FitzHugh-Nagumo, since there is no second zero to locate.

3.2.1 The reduced Evans functions

In this section, we consider the reduced Evans functions for the fast equation along the front and back of the pulse. We will show that both reduced Evans functions have no zeros with $\{\mathrm{Re}(\lambda) \geq 0\} \setminus \{0\}$, and that there is only one zero at $\lambda = 0$, associated with the front.

Recall that, along the front, to leading order we have $h \equiv 1$. As a result, the reduced, fast PDE that governs the dynamics of the front is given by

$$v_t = v_{\xi\xi} - cv_\xi + Rv^2(1-v) - v. \tag{3.10}$$

As mentioned above, this is just the bistable equation, and the front is the heteroclinic connection between 0 at $-\infty$ and $v^+(1)$ at $+\infty$. Up to rescaling, this is also the equation that governs the dynamics of the front of the pulse for the Fitzhugh-Nagumo equation. Its Evans function was analyzed in detail in [Jon84], and we summarize those results in the following proposition.

Proposition 3.2. *[Jon84] Let $D_F(\lambda)$ denote the reduced Evans function that one obtains from the stability analysis of the heteroclinic front of equation (3.10). Then D_F is analytic in $\tilde{\Omega}$ and*

1. $D_F(0) = 0$

2. $D_F(\lambda) \neq 0$ *for all* $\lambda \in \tilde{\Omega} \setminus \{0\}$.

In [Jon84], it was also shown that $\frac{d}{d\lambda} D_F(\lambda)|_{\lambda=0} > 0$, although we will not need that fact here. However, we do need that the derivative of the Evans function at 0 is non-zero, for simplicity of the eigenvalue. We remark that the b in the definition of $\tilde{\Omega}$ may need to be chosen slightly smaller than above, in order for this proposition to hold.

Next, consider the reduced PDE for the back,

$$v_t = v_{\xi\xi} - cv_\xi - v(2v-1)^2, \tag{3.11}$$

where c is the wavespeed that was selected in the analysis of the front (see equation (2.6) for $h = 1$). As mentioned above, this is the generalized Fisher KPP equation of order 2. The back is a heteroclinic

connection between 1/2 at $-\infty$ and 0 at $+\infty$. It is asymptotic to a stable manifold at $+\infty$, but a center manifold at $-\infty$, where it decays only algebraically. In addition, the essential spectrum of the associated linearized operator is contained in a parabolic region of the left half plane that touches the imaginary axis at the origin. As a result, the stability analysis of the back and construction of the associated reduced Evans function is a bit more subtle. However, this analysis has been carried out in [WXY06], and we collect the relevant results.

Proposition 3.3. *[WXY06] Let $D_B(\lambda)$ denote the reduced Evans function that one obtains from the stability analysis of the heteroclinic solution of equation (3.11). Then*

1. *D_B is analytic in $\tilde{\Omega}$*

2. *$D_B(\lambda) \neq 0$ for all $\lambda \in \tilde{\Omega}$.*

Again, it may be necessary to take b in the definition of $\tilde{\Omega}$ to be slightly smaller than above.

It may be surprising that the derivative of the heteroclinic solution does not lead to a zero of the reduced Evans function at the origin. This is because the Evans function in [WXY06] is constructed using the strong unstable eigenvalue at $-\infty$. Since the wave decays only algebraically there, it is asymptotic to the weak unstable direction and, therefore, does not contribute a zero. See [WXY06] Theorem 2.1 and Lemma 4.1 for more details.

3.2.2 Approximation of eigenvalues

We now show that any zero of the Evans function $D(\lambda)$ in $\tilde{\Omega}$ must be near the unique zero of $D_F(\lambda)$ and $D_B(\lambda)$ in that region, $\lambda = 0$. Let B_δ denote the ball of radius δ at 0, where δ is chosen sufficiently small so that $B_\delta \subset \tilde{\Omega}$, and let $G = \tilde{\Omega} \setminus B_\delta$.

Lemma 3.4. *$D(\lambda) \neq 0$ for all $\lambda \in G$.*

Proof First, we note that we need only consider a bounded region within G, say $\hat{G} = \{\lambda \in G : |\lambda| < M\}$ for some fixed M that is independent of ϵ. This can be shown using a scaling argument [San02].

Fix $\lambda \in \hat{G}$ and consider $\zeta(\xi, \lambda)$ and $\eta(\xi, \lambda)$, defined in equations (3.6) and (3.8). We will track ζ around the pulse until ξ is sufficiently large and then show that it cannot be orthogonal to η.

The main idea is to show that, in the absence of an eigenfunction for the reduced fast flows, the strong unstable direction is always an attractor for the evolution of ζ. As a result, if $\lambda \notin \hat{G}$, then the unstable directions completely determines the evolution of ζ, and we can use it to track the evolution around the pulse and show it cannot be orthogonal to η. This argument will be similar to that of [Jon84], and so some details will be omitted.

In order to follow $\zeta(\xi, \lambda)$ around the pulse, we must track its evolution according to equation (3.2). To make this more precise, one must couple the traveling wave system (2.1) to equation (3.2) and track the combined solution $((V(\xi), W(\xi), H(\xi)), (p(\xi), q(\xi), r(\xi)))$. However, for our purposes it is sufficient to refer only to system (3.2). In addition, in [Jon84] the wave was parameterized by $\theta \in S^1$, but we will not discuss this further here.

First, we track ζ along the fast front. If $v_F(\xi)$ and $w_F(\xi)$ denote the leading order fast pulse along the front, then the eigenvalue problem associated with equation (3.10) is

$$\begin{aligned} v_\xi &= w \\ w_\xi &= [\lambda - 2Rv_F(1-v_F) + Rv_F^2 + 1]v + cw. \end{aligned} \tag{3.12}$$

The reduced Evans function along the front is defined by $D_F(\lambda) = \zeta_F(\xi,\lambda)\cdot\eta_F(\xi,\lambda)$, where ζ and η are defined analogously to equations (3.6) and (3.8).

To leading order, $\zeta(\xi,\lambda) = (\zeta_F(\xi,\lambda),0)$ and $\eta(\xi,\lambda) = (\eta_F(\xi,\lambda),0)$. In other words, the components of the full Evans function are just the inclusions in $\mathbb{R}^3$ of their reduced counterparts. Therefore, to leading order, the reduced equation can be used to track the evolution of ζ along the front of the wave.

We are really only interested in the direction of the vector $\zeta(\xi,\lambda)$, which can be studied using the projectivized version of (3.2). To that end, define $(a,b) := \pi(p,q,r) = (q/p, r/p)$. Thus, $\pi : \{(p,q,r)\in\mathbb{C}^3 : p \neq 0\} \to \mathbb{CP}^2$. The evolution of (a,b) is governed, to leading order, by

$$\begin{aligned} a' &= [\lambda - 2RHV(1-V) + RHV^2 + 1] + ca - RV^2(1-V)b - a^2 \\ b' &= -\frac{\lambda}{c}b - ab. \end{aligned} \tag{3.13}$$

The eigenvector associated with the unique largest eigenvalue of an ODE always corresponds to a stable fixed point of the corresponding projectivized system. If we fix λ and consider the "frozen" version of equation (3.13), where ξ is fixed on the right hand side, then the projectivized version of that eigenvector is an attractor for the system. Taking a union over all ξ in some interval, for example, we would obtain an attractor for the evolution of (3.13) in that interval. (Note: this fact relies on the compactness of $\hat{G}$.) If we then let $\hat{\zeta}$ denote the projectivized version of ζ, that attractor would govern the evolution of $\hat{\zeta}$ along that interval.

We could similarly construct the projectivized version of the reduced equation (3.12). The unstable direction is an attractor for $\hat{\zeta}_F$ as it follows the front. For $\lambda \in \hat{G}$, we know the reduced system does not have an eigenvalue, and so $\hat{\zeta}_F$ will approach the unstable direction as $\xi \to +\infty$. Thus, when the pulse enters a neighborhood of the invariant slow manifold, $\hat{\zeta}(\xi,\lambda)$ will be equal, to leading order, to the direction of the unstable fast fiber of the manifold.

Next, we need to track $\hat{\zeta}$ down along the slow manifold until the pulse enters a neighborhood of the knee. Using the projectivized equations associated with the fast flow for any fixed $h \in (4/R, 1]$, one sees that the union of the unstable eigenvectors associated with the fixed points $(v^+(h),0)$ of equation (2.2) is an attractor. As a result, as $\hat{\zeta}$ follows the first slow piece of the pulse, it will remain close to the direction of the unstable fibers of the slow manifold, until it enters a neighborhood of the knee.

Now we must track $\hat{\zeta}$ around the knee. For $\lambda \in \hat{G}$, the presence of the knee does not pose any additional complications, and the analysis follows as in [Jon84]. This is because, when $(V,H) \sim (1/2, 4/R)$ at the knee, equation (3.2) is hyperbolic for $\lambda \neq 0$. There is still a unique largest eigenvalue, and $\hat{\zeta}$ will be attracted to the direction of its corresponding eigenvector.

The analysis of the evolution of $\hat{\zeta}$ along the back is similar to that of the front, above. The key fact is that, when $\hat{\zeta}$ emerges from a neighborhood of the knee, it will be close to the strong unstable direction. Since this direction corresponds to the unstable fiber of the (normally hyperbolic) center manifold, it will perturb smoothly. In other words, it is a tangent vector living in the tangent space of the traveling wave (which is $\mathcal{O}(\epsilon^{2/3})$ close to the leading order wave) and its direction is C^1 $\mathcal{O}(\epsilon)$ close to the leading order strong

unstable direction. Since it is this direction that is used to construct the Evans function in [WXY06], we can then use those results to conclude that any zero of the full Evans must be near a zero of the reduced Evans function.

Because the reduced equation, the linearization of the generalized KPP equation, does not have a eigenvalue in $\hat{G}$, $\hat{\zeta}$ must be $\mathcal{O}(\epsilon)$ close to the direction of the unstable fibers as the pulse enters a neighborhood of the slow invariant manifold. Thus, we can follow it up along the slow manifold S_l and conclude that it is not orthogonal to $\hat{\eta}(\xi, \lambda)$ when the pulse enters a neighborhood of the fixed point $(0, 0, 1)$. Because the $\hat{\zeta}$ and $\hat{\eta}$ determine the directions of the vectors ζ and η, this proves that ζ and η are not orthogonal, as well. $\square$

3.2.3 Winding number calculation

We know from the previous section that any potential unstable eigenvalues must lie in B_δ, the ball of radius δ at the origin. Let $K = \partial B_\delta$ denote the boundary of that ball, and chose δ sufficiently small so that zero is the only eigenvalue of either reduced fast system that is contained in B_δ. We will compute the winding number of $D(\lambda)$ along K and show that it is one. This will show that there is exactly one zero of the Evans function in $\tilde{\Omega}$, which implies that there is exactly one eigenvalue of geometric and algebraic multiplicity one in $\tilde{\Omega}$ [AGJ90]. Since we know there must exist an eigenvalue at $\lambda = 0$, it is the only one. This will complete the proof of theorem 3.1. We remark that, again, this argument is similar to that of [Jon84], and so we do not include all of the details here. As above, we must check that the presence of the knee does not affect the winding number.

Note that an analytic extension of the Evans function is defined for all $\lambda \in B_\delta \cup K$, uniformly in ϵ, and that it is nonzero on K. Any zero inside B_δ necessarily corresponds to an eigenvalue only if it is in $\Omega \cup \{0\}$.

In the previous section, it was shown that the projectivized equations can be used to track $\hat{\zeta}$ around the pulse. If we take an element $(q/p, r/p) \in \mathbb{CP}^2$, then we can associated it with an element in $\mathbb{C}^3$ using $\pi^{-1}(q/p, r/p) = (1, q/p, r/p)$, which is just a normalized version of the vector (p, q, r). When computing the winding number we will need not only the direction of the vector, but its amplitude as well. One can directly check that, for any ξ such that $p(\xi, \lambda) \neq 0$,

$$\zeta(\xi, \lambda) = p(\xi, \lambda)[\pi^{-1}(\hat{\zeta})](\xi, \lambda).$$

The Evans function is independent of ξ, and so we can evaluate the expression on the right hand side of equation (3.9) at any value of ξ we choose. It is convenient to pick some sufficiently large value of ξ, denoted by T_4. One can then show that $W(D(K)) = W(p(T_4, K))$. The proof of this fact follows closely that in [Jon84], and so we do not repeat it here.

Let T_0 be the value of ξ for which the underlying wave exits a neighborhood of $(0, 1)$, T_1 be the value at which it enters a neighborhood of $(v^+(1), 1)$, T_2 be the value at which it exits a neighborhood of $(1/2, 4/R)$, and T_3 be the value at which it enters a neighborhood of $(0, 4/R)$. Similar to the previous section, we will track the evolution of $p(\xi, \lambda)$ around the underlying pulse and evaluate the winding numbers $W(p(T_i, K))$ for $i = 0, \ldots, 4$, showing

1. $W(p(T_0, K)) = 0$
2. $W(p(T_1, K)) = 1$
3. $W(p(T_2, K)) = 1$

4. $W(p(T_3, K)) = 1$

5. $W(p(T_4, K)) = 1$.

Note that, in [Jon84], it was shown $p(T_i, K) \neq 0$ for $i = 0, 4$. In other words, as p moves along the pulse, the corresponding winding number increases by one only as it moves along the front, due to the eigenvalue of the reduced system there. Along the rest of the wave, it remains constant.

The proof essentially follows from the results in [Jon84]. The only thing one needs to check, due to the presence of the knee, is that $W(p(T_2, K)) = 1$. This would follow if $p(\xi, \lambda) \neq 0$ for all $\xi \in [T_1, T_2]$, uniformly for λ near zero. This is because one could then construct a homotopy between $p(T_1, K)$ and $p(T_2, K)$ to show that their winding numbers are equal.

Consider the projectivized system (3.13) near the knee, *i.e.* for $(V, H) \sim (1/2, 4/R)$:

$$a' = \lambda + ca - \frac{R}{8}b - a^2$$
$$b' = -\frac{\lambda}{c}b - ab.$$

The three fixed points of this system are $(a^+(\lambda), 0)$, $(a^-(\lambda), 0)$, and $(-\lambda/c, -8\lambda^2/Rc)$, where $a^\pm = (c \pm \sqrt{c^2 + 4\lambda})/2$. These correspond to the unstable, stable, and center directions of the slow manifold, respectively. As $\lambda \to 0$, $(a^-, 0)$ and $(-\lambda/c, -8\lambda^2/Rc)$ coincide, but the remaining fixed point remains separate, uniformly in λ. It is this direction that defines the attractor that $\hat{\zeta}$ follows as it moves along the wave. Since these fast unstable directions always point along vectors with nonzero p component, this shows that $p(\xi, \lambda) \neq 0$ for all $\xi \in [T_1, T_2]$, uniformly for λ near zero, just as in [Jon84].

In other words, the evolution of $\hat{\zeta}$, and hence the winding number, is determined primarily by the behavior of the strong unstable direction to which it is attracted. Since we have shown that this direction remains unique despite the nonhyperbolicity at the knee, the winding number calculation in essentially the same as in [Jon84].

By continuing to follow ζ along the pulse, we arrive at $W(p(T_4, K)) = W(D(K)) = 1$. This proves that there is only one zero of the Evans function in $\tilde{\Omega}$, and since we know there exists a zero at the orgin it must be the only one. This concludes the proof of the spectral stability of the wave.

4 Spatially periodic waves

We now briefly remark on the existence and biological relevance of spatially periodic waves, which will be the subject of future work.

Recall from equations (2.6) and (2.7) that the fast jumps exist for explicitly computable values of the wavespeed. If we can find a c_{per} and an $h_{per} \in (4/R, 1)$ such that a fast jump exists at h_{per} from $v = 0$ at $\xi = -\infty$ to $v = v^+(h_{per})$ at $\xi = +\infty$, and $c_{per} = c(h_{per}, R) > \sqrt{2}/2$, then we would be able to construct a leading order periodic solution consisting of the following four pieces:

1. A fast jump from $(0, 0, h_{per})$ to $(v^+(h_{per}), 0, v^+(h_{per}))$, which is given explicitly in equation (2.6), with $c_{per} = c(R, h_{per})$

2. Slow decay along S_r

3. A fast jump from $(1/2, 0, 4/R)$ to $(0, 0, 4/R)$, with $c_{per} = c(R, h_{per})$

4. Slow growth along S_l back to $(0, 0, h_{per})$.

Note we require that $c_{per} > \sqrt{2}/2$ so that the second fast jump must occur at the knee along the center manifold. If $c_{per} \leq \sqrt{2}/2$, then the second fast jump would leave the slow manifold along an unstable manifold, which is not what happens in cardiac dynamics, as discussed in section 1.

In figure 2, we see that such an orbit is possible only if $R > 25/4$. Otherwise, the first fast jump will necessarily occur for a value of the wavespeed less than $\sqrt{2}/2$. If $R > 25/4$, then a first fast jump with sufficiently large wavespeed exists for $h > 25/4R$. As a result, there exists at leading order a family of periodic orbits, one for each $h_{per} \in (25/4R, 1)$.

Regarding the investigation of the persistence of this family, for $\epsilon > 0$, we expect that a combination of the techniques used to prove the existence of a family of spatially periodic solutions to the FitzHugh-Nagumo equation [Car77] and the blow-up, used in this paper, will be applicable. To investigate stability, it is possible that the theory developed in [Gar97, SS01] will apply. In those papers, the authors investigated the linear stability of families of periodic waves of reaction diffusion equations that are close to a homoclinic orbit – at least for sufficiently large period – and, in particular, applied their results to the family of periodic solutions of the FitzHugh-Nagumo equation.

Periodic solutions are of biological interest because they represent a beating heart. In cardiac models, the stability of these periodic waves cannot persist indefinitely as the period is shortened. Even the ODE model suffers a period-doubling bifurcation as the pacing period is shortened. The bifurcation in the PDE context is more complicated than simple period doubling–see for example [EK02, EK06]. We plan to study this bifurcation in a subsequent publication.

5 Acknowledgments

M.B. wishes to thank Björn Sandstede for helpful discussions on the extension of the Evans function into the essential spectrum and Steve Schecter for bringing [WXY06] to her attention. M.B., C.J., and M.W. would like to thank the Mathematical Sciences Research Institute in Berkeley, CA, for their hospitality during the spring of 2007, while part of this work was completed. The research of M.B. was partially supported under NSF grant number DMS-0602891. The research of C.J. was partially supported under NSF grant number DMS-0410267. The research of D.S. was partially supported by NSF grant number PHY-0549259 and NIH grant number 1R01-HL-7283.

References

[AGJ90] J. Alexander, R. Gardner, and C. Jones. A topological invariant arising in the stability analysis of traveling waves. *J. reine angew. Math.*, 410:167–212, 1990.

[BJ89] P. W. Bates and C.K.R.T. Jones. Invariant manifolds for semilinear partial differential equations. *Dynamics Reported*, 2:1–38, 1989.

[BR77] G. W. Beeler and H. Reuter. Reconstruction of the action potential of ventricular myocardial fibres. *J. Physiol.*, 268:177–210, 1977.

[Car77] G. A. Carpenter. A geometric approach to singular perturbation problems with applications to nerve impulse equations. *J. Differential Equations*, 23(3):335–367, 1977.

[CS06] J. W. Cain and D. G. Schaeffer. Two-term asymptotic approximation of a cardiac restitution curve. *SIAM Rev.*, 48(3):537–546 (electronic), 2006.

[EK02] B. Echebarria and A. Karma. Instability and spatiotemporal dynamics of alternans in paced cardiac tissue. *Phys. Rev. Lett.*, 88(208101), 2002.

[EK06] B. Echebarria and A. Karma. Amplitude equation approach to spatiotemporal dynamics of cardiac alternans. *To appear in Phys. Rev. E.*, 2006.

[Eva73] J. W. Evans. Nerve axon equations. III. Stability of the nerve impulse. *Indiana Univ. Math. J.*, 22:577–593, 1972/73.

[Fen71] N. Fenichel. Persistence and smoothness of invariant manifolds for flows. *Ind. Univ. Math. J.*, 21:193–226, 1971.

[Fen79] N. Fenichel. Geometric sinfular perturbation theory for ordinary differential equations. *J. of Diff. Eqs.*, 31:53–98, 1979.

[Gar97] R. A. Gardner. Spectral analysis of long wavelength periodic waves and applications. *J. Reine Angew. Math.*, 491:149–181, 1997.

[GZ98] R. A. Gardner and K. Zumbrun. The gap lemma and geometric criteria for instability of viscous shock profiles. *Comm. Pure Appl. Math.*, 51(7):797–855, 1998.

[Hen81] D. Henry. *Geometric Theory of Semilinear Parabolic Equations*. Springer-Verlag, Berlin, 1981.

[HN60] O. F. Hutter and D. Noble. Rectifying properties of heart muscle. *Nature*, 188(495):495–497, November 1960.

[JK94] C. K. R. T. Jones and N. Kopell. Tracking invariant manifolds with differential forms in singularly perturbed systems. *J. Differential Equations*, 108(1):64–88, 1994.

[JKL91] C. K. R. T. Jones, N. Kopell, and R. Langer. Construction of the FitzHugh-Nagumo pulse using differential forms. In *Patterns and dynamics in reactive media (Minneapolis, MN, 1989)*, volume 37 of *IMA Vol. Math. Appl.*, pages 101–115. Springer, New York, 1991.

[Jon84] C. K. R. T. Jones. Stability of the traveling wave solution of the fitzhugh-nagumo system. *Transactions of the AMS*, 286(2):431–469, 1984.

[Jon94] C. K. R. T. Jones. Geometric singular perturbation theory. In R. Johnson, editor, *Dynamical Systems*, volume 1609 of *Lecture Notes in Mathematics*, pages 44–118. Springer-Verlag, Berlin, 1994.

[Kap99] T. J. Kaper. An introduction to geometric methods and dynamical systems theory for singular perturbation problems. *Proceeding of Symposia in Applied Mathematics*, 56:85–131, 1999.

[Kar93] A. Karma. Spiral breakup in model equations of action potential propagation in cardiac tissue. *Phys. Rev. Lett.*, 71(7):1103–1106, 1993.

[Kar94] A. Karma. Electrical alternans and spiral wave breakup in cardiac tissue. *Chaos*, 4(3):461–472, 1994.

[KS98] T. Kapitula and B. Sandstede. Stability of bright solitary-wave solutions to perturbed nonlinear schrodinger equations. *Physica D*, 124:58–103, 1998.

[KS01] M. Krupa and P. Szmolyan. Extending geometric singular perturbation theory to nonhyperbolic points - fold and canard points in two dimensions. *SIAM J. Math. Anal.*, 33(2):286–314, 2001.

[LR91] C. H. Luo and Y. Rudy. A model of the ventricular cardiac action potential. Depolarization, repolarization, and their interaction. *Circ. Res.*, 68:1501–1526, 1991.

[LR94] C. H. Luo and Y. Rudy. A dynamic model of the cardiac ventricular action potential. I. Simulations of ionic currents and concentration changes. *Circ. Res.*, 74:1071–1096, 1994.

[MS03] C. C. Mitchell and D. G. Schaeffer. A two-current model for the dynamics of cardiac membrane. *Bulletin of Mathematical Biology*, 65:767–793, 2003.

[Nob62] D. Noble. A modification of the Hodgkin-Huxley equations applicable to Purkinje fibre action and pace-maker potentials. *J. Physiol.*, 160:317–352, 1962.

[PK06] N. Popović and T. J. Kaper. Rigorous asymptotic expansions for critical wave speeds in a family of scalar reaction-diffusion equations. *J. Dynam. Differential Equations*, 18(1):103–139, 2006.

[San02] B. Sandstede. Stability of travelling waves. In *Handbook of dynamical systems, Vol. 2*, pages 983–1055. North-Holland, Amsterdam, 2002.

[SS01] B. Sandstede and A. Scheel. On the stability of periodic traveling waves with large spatial period. *Journal of Differential Equations*, 172:134–188, 2001.

[WXY06] Y. Wu, X. Xing, and Q. Ye. Stability of travelling waves with algebraic decay for n-degree Fisher-type equations. *Discrete Contin. Dyn. Syst.*, 16(1):47–66, 2006.

[Xin00] J. Xin. Front propagation in heterogeneous media. *SIAM Rev.*, 42(2):161–230 (electronic), 2000.